

# Finite Element Updating Method for High-Precision Space Reflector Model Using Multiobjective Optimization

By Nozomu KOGISO<sup>1)</sup>, Takayuki OKABE<sup>1)</sup>, Hiraku SAKAMOTO<sup>2)</sup> and Hiroaki TANAKA<sup>3)</sup>

<sup>1)</sup>Department of Aerospace Engineering, Osaka Prefecture University, Sakai, Japan

<sup>2)</sup>Department of Mechanical and Aerospace Engineering, Tokyo Institute of Technology, Tokyo, Japan

<sup>3)</sup>Department of Aerospace Engineering, National Defense Academy of Japan, Yokosuka, Japan

(Received July 20th, 2015)

This study proposes a finite element updating method using multiobjective optimization to consider multiple experimental conditions for estimating parameters. The method aims to minimize the root-mean-square (RMS) error of the deformation shape between the finite element analysis and experimental results. The proposed method is applied to the bread board model (BBM) of a tension-stabilized space reflector consisting of hoop cables and radial ribs, in which the rib is deformed into the prescribed shape by the cable tensions generated on deployment. The design requirement is to deform the rib into the prescribed shape by applying appropriate tension loads to the radial and hoop cables. Under actual conditions, the deformation shape deviates from the ideal shape because of uncertainties. Therefore, it is necessary to estimate the physical parameters with high accuracy, through a geometrically nonlinear finite element analysis, in order to investigate their effect on the deformation shape. To efficiently estimate the physical parameters, the satisficing trade-off method (STOM) is adopted as the multiobjective optimization method. Through numerical examples, the validity of the proposed method is demonstrated by comparing the analytical deformation shapes with experimental results.

**Key Words:** Finite Element Updating, High-Precision Space Structure, Multiobjective Optimization, Satisficing Trade-Off Method

## 1. Introduction

Space antennas for space exploration missions have to be lightweight with large aperture areas and high surface shape accuracy.<sup>1)</sup> To satisfy these requirements, a large-scale highly precise tension-stabilized space reflector, consisting of hoop cables and radial ribs, was proposed<sup>2)</sup> as shown in Fig. 1. In this structure, the ribs are arranged radially from a central hub and simply supported at the hub. They are originally straight in the folding position and, on deployment, undergo bending deformations under the tensions of the hoop and tie cables. The dimensions of the ribs are determined such that the deformation shape will be close to the ideal parabolic shape.

The structural design of the reflector was verified using a one-dimensional rib model, as shown in Fig. 2, that consists of a

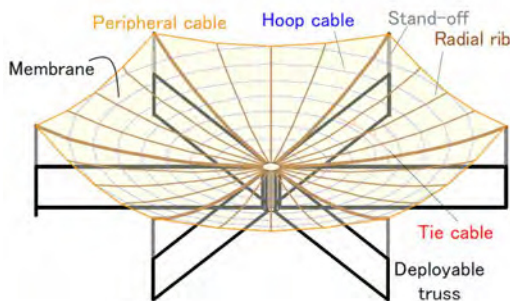


Fig. 1. Reflector consisting of radial ribs and hoop cables as large-scale highly precise tension-stabilized space structure.

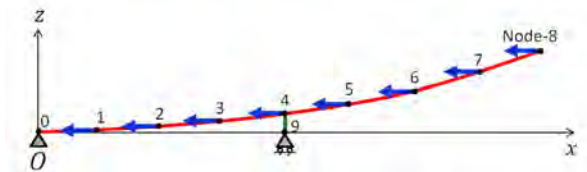
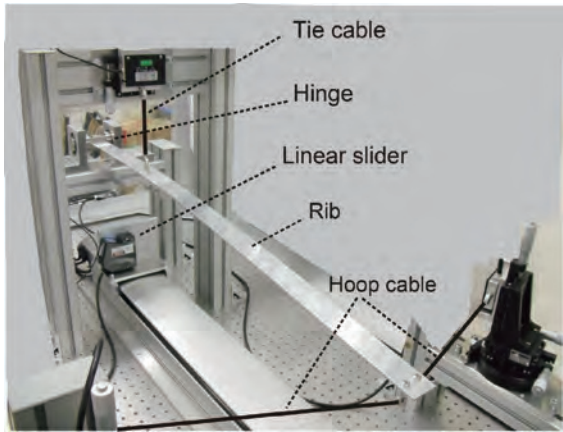


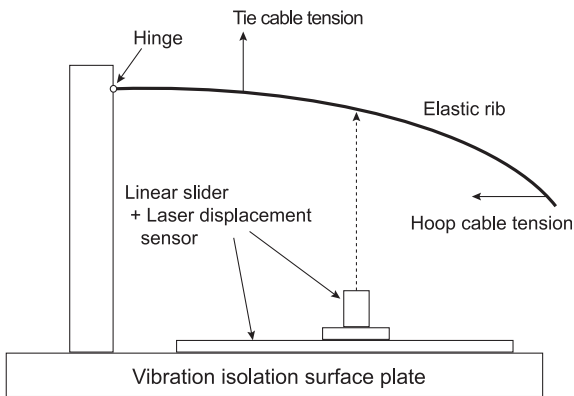
Fig. 2. Simplified one-dimensional structural model of single rib of reflector.

single rib of the reflector and a cable element representing the tie cable.<sup>2)-4)</sup> The root of the rib is simply supported, and the lower end of the tie cable is fixed in the vertical direction and free to move in the longitudinal direction. The hoop cable tension is modeled as a concentrated nodal load that deforms the rib from its original straight form into the ideal parabolic shape. The deformation transfers the tension force to the tie cable as a reaction force.

In order to ensure that the ideal deformed shape is obtained, a highly accurate numerical analysis, such as a structural nonlinear finite element analysis, has to be conducted on the structure. To reduce the errors in the analysis, the structural parameters, such as stiffness and internal stress, have to be estimated precisely. For this purpose, some of the authors proposed a parameter estimation method for the tension-stabilized structure.<sup>5)</sup> They applied finite element updating, which is usually employed in linear finite element analyses,<sup>6),7)</sup> to the geometrically nonlinear finite element analysis required for the structure. In tension-stabilized space structures, the balance of internal forces determines the structural shape, which in turn influences the distribution of the internal forces; therefore, the internal forces and deformation have to be solved simultaneously. The structural parameters are estimated by the finite ele-



(a) Photograph of experimental system



(b) Schematic of experimental system

Fig. 3. Overview of experimental system.

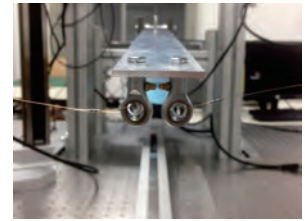
ment updating method using the results of a shape measurement experiment. The present experimental setup, shown in Fig. 3, is the simplest representation of the tension-stabilized structure and consists of only one layer of hoop cables as the bread board model (BBM). As shown in Figs. 4 (a) and 4 (b), the cables are connected to the rib through rod end elements to avoid cable twisting, and the other ends of the cables are connected to load cells to measure the cable tensions. The root of the rib is simply supported using a hinge, as shown in Fig. 4 (c), which consists of ball bearings to reduce the rotational friction. However, some friction still exists and have adverse effect on the rib deflection.

In our previous study,<sup>5)</sup> the deformation error between the experimental and finite element method (FEM) results was reduced by selecting parameters with high sensitivity to the rib deformation as the updated parameters. However, the cable tensions estimated by the finite element updating were very different from the experimental values, even at low deformation errors. It was found that the additional experiments that applied known perturbations to the structure were efficient in reducing the errors.<sup>5)</sup> Moreover, the previous research concluded that an efficient updating method that considers multiple experimental conditions is required for accurate parameter estimation.

This study proposes a new finite element updating method using the multiobjective optimization approach, for estimating the structural parameters with high accuracy. The satisficing trade-off method (STOM)<sup>8)</sup> is adopted as the multiobjective optimization method. STOM can provide a single, highly accurate Pareto solution regardless of the shape of the Pareto set.



(a) Rod end connecting tie cable and rib



(b) Rod end connecting hoop cables and rib



(c) Root hinge

Fig. 4. Details of experimental system.

STOM transforms multiple objective functions into the equivalent single objective function by introducing an aspiration level for each objective function value, according to the user's preference. When the optimization problem is formulated as a continuous design variable problem and the objective and constraint functions are differentiable with respect to the continuous design variables, a computationally efficient mathematical programming method for a single objective optimization problem can be adopted. Therefore, STOM has been widely applied to various engineering design problems.<sup>9)</sup> In addition, part of the authors developed robust multiobjective optimization<sup>10)</sup> and reliability-based multiobjective optimization methods<sup>11)</sup> considering the uncertainties in STOM.

The rest of the paper is organized as follows. Section 2 introduces the experimental model and the deformation measurement. The corresponding finite element model is introduced in section 3. Then, section 4 describes the proposed finite element updating method using multiobjective optimization. In addition, STOM is briefly introduced. The parameter estimation results are illustrated in section 5 and finally, conclusions are remarked.

## 2. Experimental Model and Deformation Measurement

The simplified reflector shown in Fig. 3 consists of a single rib, on which a tension load is applied by a tie cable and a pair of hoop cables. The rib is made of aluminum alloy and has a length 1040 mm and a uniform rectangular cross section of 40 mm width and 3 mm thickness. The Young's modulus of the rib is obtained from a simple bending experiment as 69.87 GPa. The Young's modulus and the rib dimensions are used in the analysis as constant values, not as estimating parameters.

The cables are made of phosphor bronze and have a diameter of 0.3 mm. The tie and hoop cables are connected to the rib through rod ends at the locations 300 mm and 1000 mm, respectively, from the hinge center. The other ends of the cables

Table 1. Load cases.

Case	1	2	3	4
Tie cable tension [N]	6.814	7.622	8.418	9.223
Hoop cable tension [N]	34.97	29.94	24.99	19.97

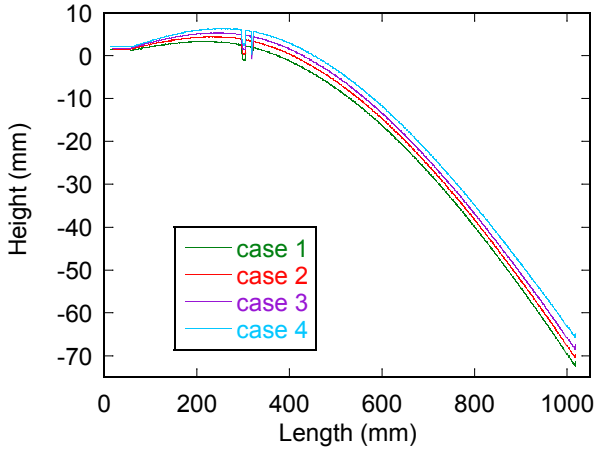


Fig. 5. Deformation obtained by experiment.

are fixed to load cells placed on stages, to measure the tension. The hoop cables are connected to the rib at 15° inclined to the root direction.

The rib connected to the hinge is deformed by applying appropriate tensions to the connected cables. For stable deformation of the rib, the tension is applied in three steps as follows:

**step 1** Only the tie cable is connected to the rib, that is, the rib is supported only by the hinge and the tie cable and is deformed by its own weight.

**step 2** The hoop cables are connected to the rib. A negligibly small tension is applied to the hoop cables to prevent them from slacking. In this step, the hoop cable is declined because the rib is not fully deformed in the down direction yet.

**step 3** The rib is deformed by applying the prescribed tensions to all three cables. To achieve this, each hoop cable is pulled horizontally along the cable arranging direction by sliding the stage on which the load cell connected to the other end of the hoop cable is fixed. The tensions in both the hoop cables are adjusted simultaneously by changing the stage positions. Then, the tie cable tension is adjusted by the stage connected at its other end.

In each load case, the rib deformation is measured by a laser displacement sensor located on a linear slider with a 0.8 m stroke.

By the above-mentioned steps, the different cable tensions listed in Table 1 are applied to deform the rib under four different load cases.

The deformation of the rib in the four cases are shown in Fig. 5. The largest tip displacement is observed in load case 1 because the hoop cable tensions are highest in this case. On the other hand, the tie cable tension is lowest among the four cases. This is because the hoop cable tension pulls the rib in the hinge direction as well as downward in the vertical direction. Hence, at the location of the tie cable, the rib is slightly deformed upward in the vertical direction, reducing the tie cable tension. The four load cases are used to estimate the parameters in the finite element updating. As uneven deformation is caused near

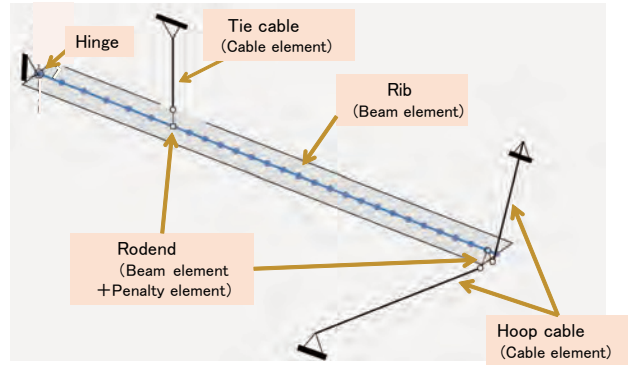


Fig. 6. Finite element model of one-dimensional simplified rib model.

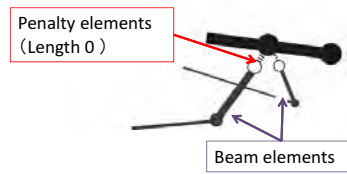


Fig. 7. FEM model at rod end element.

the 300 mm location by the tie cable connecting bolt as shown in Fig. 4 (a), that section is not used in the finite element updating.

### 3. FEM Model of Rib Structure

The FEM model of the rib structure is shown in Fig. 6. The rib is modeled using beam elements, and the cables are modeled by cable elements, which, unlike rod elements, do not support compression loads. The rod ends that connect the cables to the rib are modeled using beam elements. In addition, a penalty element, which has zero length and is rigid under bending, is included at each connecting point between the rib and the cables. These elements are used to simulate the deformation of the rod end such that the connecting angle is always perpendicular to the rib, as illustrated in Fig. 7. The rib is equally divided into 28 elements, and the entire structure is modeled by 36 elements and 37 nodes.

As a boundary condition, the ends of the cables opposite the rod ends are fixed. The cable tensions are obtained as the reaction forces and are compared with the experimental results. The hinge of the rib is simply supported. However, it is found from the experimental results that the hinge has a small rotational friction. In order to estimate this unknown friction, it is simulated by applying an equivalent moment at the hinge. The magnitude of the moment is estimated through the FE updating.

The FEM analysis is performed with the same conditions as the experiment using the three-step loading described in the previous section.

### 4. Finite Element Updating Using Multiobjective Optimization

Finite element updating is a method for estimating several parameters accurately by changing their values to reduce the difference in structural responses between the finite element analysis and experimental results. Usually, an optimization method is adopted to minimize the difference, and a root-mean-square

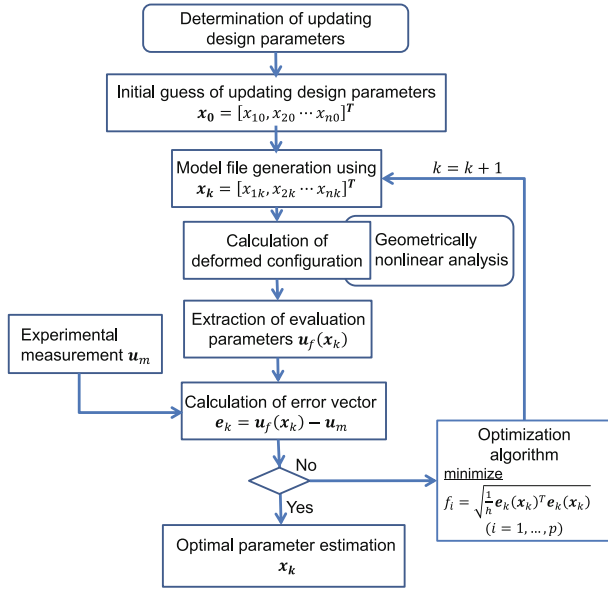


Fig. 8. Flowchart of finite element model updating using STOM.

(RMS) error is defined in terms of the estimating parameters as the objective function. This study considers multiple experimental conditions for estimating the parameters. Conventionally, the single scalar value to minimize is introduced by summarizing each RMS error for each experimental condition with weight coefficient. However, it is difficult to obtain the desired solution that minimizes RMS error by controlling the weight coefficients. Therefore, a multiobjective optimization method is adopted in order to find the parameter values that minimizes the maximum value of the RMS errors corresponding to the multiple experimental conditions.

The procedure of finite element updating using multiobjective optimization is shown in Fig. 8 and summarized as follows:

1. First, the updating parameters are denoted as  $\mathbf{x}_i = [x_1, x_2, \dots, x_n]^T$ . Set  $i = 0$  for the initial estimate value  $\mathbf{x}_i$ . In this study, the tensions applied at tie and hoop cables are adopted as estimated parameters. In addition, the moment at the root hinge that is introduced to simulate the unknown friction at the hinge is also used as estimated parameters. Since the parameters are independent for four load cases, the number of the estimated parameters is twelve.
2. The rib deformation  $\mathbf{u}_f^{(k)}(\mathbf{x}_i)$  is evaluated by the geometrically nonlinear finite element analysis, where  $k$  corresponds to the experimental case.
3. The residual  $\mathbf{e}_i^{(k)}$  is evaluated as the difference between the deformation shape  $\mathbf{u}_f^{(k)}(\mathbf{x}_i)$  calculated by the analysis and that obtained experimentally,  $\mathbf{u}_m$ .

$$\mathbf{e}_i^{(k)}(\mathbf{x}_i) = \mathbf{u}_f(\mathbf{x}_i) - \mathbf{u}_m \quad (1)$$

4. Set the objective functions corresponding to the experimental cases as follows:

$$f_k(\mathbf{x}_i) = \sqrt{\frac{1}{2} \mathbf{e}_i^{(k)}(\mathbf{x}_i)^T \mathbf{e}_i^{(k)}(\mathbf{x}_i)} \quad (2)$$

$f_k$  corresponds to the RMS error of the rib deformation under the experimental case  $k$ . The parameters  $\mathbf{x}_i$  are updated in the multiobjective optimization step.

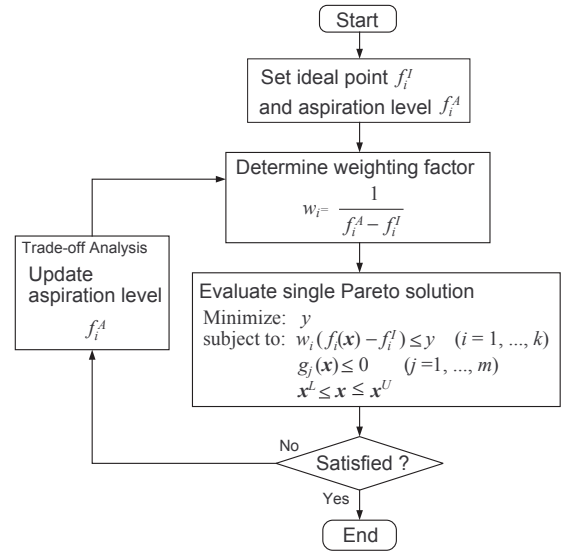


Fig. 9. Flowchart of STOM.

5. If the optimization step converges, the updated parameter is obtained. Otherwise, set  $i = i + 1$ , and go back to step 2.

#### 4.1. Multiobjective optimization method

A multiobjective optimization problem is an optimization problem with multiple objective functions.

$$\mathbf{f}(\mathbf{x}) = [f_1(\mathbf{x}), f_2(\mathbf{x}), \dots, f_k(\mathbf{x})]^T \quad (3)$$

where  $k$  is the number of objective functions,  $\mathbf{x} = (x_1, x_2, \dots, x_n)^T$  are the design variables, and  $n$  is the number of design variables.

The multiobjective optimization problem is generally formulated as follows:

$$\begin{aligned} \text{Minimize: } & \mathbf{f}(\mathbf{x}) = [f_1(\mathbf{x}), f_2(\mathbf{x}), \dots, f_k(\mathbf{x})]^T \\ \text{subject to: } & g_j(\mathbf{x}) \leq 0 \quad (j = 1, \dots, m) \\ & x_i^L \leq x_i \leq x_i^U \quad (i = 1, \dots, n) \end{aligned} \quad (4)$$

where  $g_j(\mathbf{x})$ , ( $j = 1, \dots, m$ ) are the constraint conditions and  $x_i^U$  and  $x_i^L$  are the upper and lower limits of the design variables, respectively.

This study adopts STOM as the multiobjective optimization method.<sup>8)</sup> STOM is known as an interactive optimization method that converts a multiobjective optimization problem into an equivalent single-objective optimization problem by introducing an aspiration level for each objective function value, according to the user's preference.

The algorithm of STOM is summarized in Fig. 9 and briefly described as follows:

**Step 1** Set the ideal point  $f_i^I$ , ( $i = 1, \dots, k$ ) of each objective function. The ideal point is usually determined by solving the single-objective optimization problem with only the corresponding objective function  $f_i(\mathbf{x})$ .

**Step 2** Set the aspiration level  $f_i^A$ , ( $i = 1, \dots, k$ ) of each objective function and evaluate the weight coefficient  $w_i$  as follows:

$$w_i = \frac{1}{f_i^A - f_i^I} \quad (i = 1, \dots, k) \quad (5)$$

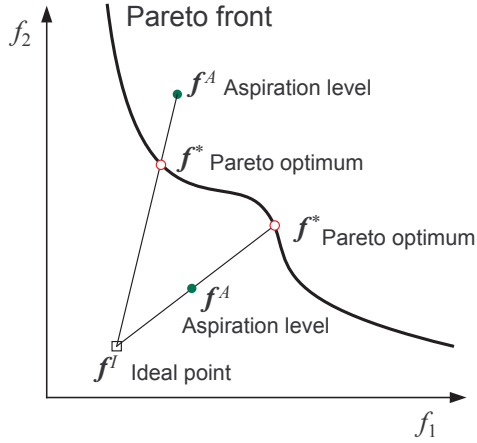


Fig. 10. Pareto solution search process of STOM.

**Step 3** Formulate the multiobjective optimization problem in Eq. (4) as a weighted Tchebyshev norm problem as follows:

$$\begin{aligned} \text{Minimize: } & \max_{i=1, \dots, k} w_i (f_i(\mathbf{x}) - f_i^I) & (6) \\ \text{subject to: } & g_j(\mathbf{x}) \leq 0 \quad (j = 1, \dots, m) \\ & x_i^L \leq x_i \leq x_i^U \quad (i = 1, \dots, n) \end{aligned}$$

**Step 4** The minimum-maximum problem in Eq. (6) is transformed into an equivalent single-objective problem by introducing a slack design variable  $y$  as follows:

$$\begin{aligned} \text{Minimize: } & y & (7) \\ \text{subject to: } & w_i (f_i(\mathbf{x}) - f_i^I) \leq y \quad (i = 1, 2, \dots, k) \\ & g_j(\mathbf{x}) \leq 0 \quad (j = 1, \dots, m) \\ & x_i^L \leq x_i \leq x_i^U \quad (i = 1, \dots, n) \end{aligned}$$

When Eq. (7) is solved using a nonlinear programming method, such as sequential programming, an accurate Pareto optimal solution is obtained efficiently in comparison with evolutionary methods.

**Step 5** If the objective function values are satisfactory, the search is completed. Otherwise, update the aspiration level  $f_i^A$ , and return to Step 2. The automatic trade-off analysis method<sup>12)</sup> known as an efficient method to update the aspiration level is available.

The weight coefficient  $w_i$  plays an important role in obtaining the Pareto solution in the direction of the aspiration level, which is directly related to the designer's preference. As shown in Fig. 10, the Pareto optimal solution is usually located on the line connecting the ideal point and the aspiration level in the objective function space, regardless of whether or not the aspiration level lies in the feasible region. On the other hand, the optimal solution is often not located on this line when some constraints are active. In that case, the designers should investigate the effect of the active constraints on the Pareto optimal solution.

Table 2. Initial and estimated parameter values and RMS error.

(a) Case 1			
		Initial	Estimated
Moment	(Nm)	0	0.0304
Tie cable tension	(N)	6.814	5.688
Hoop cable tension	(N)	46.12	46.11
RMS error	(mmRMS)	0.200	0.07287
(b) Case 2			
		Initial	Estimated
Moment	(Nm)	0	0.0209
Tie cable tension	(N)	8.566	8.120
Hoop cable tension	(N)	33.71	37.28
RMS error	(mmRMS)	0.1851	0.07287
(c) Case 3			
		Initial	Estimated
Moment	(Nm)	0	0.0149
Tie cable tension	(N)	9.368	9.134
Hoop cable tension	(N)	28.37	30.57
RMS error	(mmRMS)	0.1995	0.07286
(d) Case 4			
		Initial	Estimated
Moment	(Nm)	0	$4.57 \times 10^{-3}$
Tie cable tension	(N)	9.917	10.08
Hoop cable tension	(N)	26.75	24.63
RMS error	(mmRMS)	0.1900	0.06852

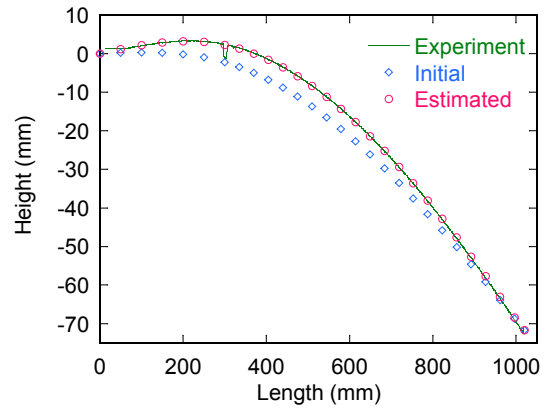


Fig. 11. Comparison of experimental result and FEM analyses using initial and updated parameters in load case 1.

## 5. Finite Element Updating Results

For the finite element updating, the four load cases listed in Table 1 are considered. The RMS errors of the rib deformation between the experiment and the analysis are defined as the objective functions in terms of the tie cable and hoop cable tensions and the moment at the root hinge, which simulates the friction at the hinge. In the STOM, the ideal point  $f_i^I$  is set to zero, which corresponds to no error, and the aspiration level  $f_i^A$  is set to 0.001 in all four cases, indicating that all the cases have the same weight.

The initial values of the updating are set as the experimental data for the cable tensions and zero for the moment. The RMS errors under the initial conditions and the estimated parameters

are listed in Table 2. The rib deformations under load case 1 from the experiment and the analysis are compared in Fig. 11. It is observed that the FEM results agree with the experimental data by the proposed updating methods.

Note that the obtained three RMS errors among four load cases are identical as 0.07287 or 0.07286 as listed in Table 2. This value is obtained by STOM corresponding to the ideal point  $f_i^I$  and the aspiration level  $f_i^A$ . If the single objective optimization method was adopted, such a desired solution could not find easily even after controlling the weighting coefficients.

Moreover, it is found that the moment at the hinge reduces the RMS error. Though the hinge ideally has no friction, the friction at the hinge has a significant effect on the rib deformation in this experiment. On the other hand, the variations in the cable tensions are small. The FEM result using the updated parameters, shown in Fig. 11, indicates that the proposed parameter estimation method works well. Because of the limitation in space, the deformations under the other load cases are not shown here, but the updating method is found to be suitable for those cases as well.

## 6. Conclusion

This study proposes a finite element updating method using multiobjective optimization to consider multiple experimental conditions for estimating parameters. As the multiobjective optimization method, the satisficing trade-off method (STOM) is adopted.

The proposed method is applied to the BBM of a tension-stabilized space reflector consisting of hoop cables and radial ribs. In this structure, the rib is deformed into the prescribed shape by the cable tensions generated on deployment. It is necessary to estimate the physical parameters of the reflector with high accuracy through a geometrically nonlinear finite element analysis in order to investigate their effect on the deformation shape.

Using numerical examples, the validity of the proposed method is confirmed by comparing the analytical deformation shapes with experimental results. In particular, the friction at the hinge support, modeled as an applied moment in the analysis, is found to have a significant effect on the rib deformation shape.

In addition, it is clarified the advantage of STOM that finds the desired Pareto solution to minimize the maximum value among the RMS errors corresponding to multiple conditions by setting the desired values of ideal point and the aspiration level.

## Acknowledgments

This study was partially supported by Institute of Space and Astronautics Sciences of the Japan Aerospace Exploration Agency (ISAS/JAXA) Strategic Research Grant and the Japan Society for the Promotion of Science (JSPS) Grants-in-Aid for Scientific Research (KAKENHI) Grant Number 26249131.

## References

- 1) Higuchi, K., Kishimoto, N., Meguro, A., Tanaka, H., Yoshihara, M. and Iikura, S.: Structure of High Precision Large Deployable Re-

- 2) Tanaka, H., Akita, T., Kogiso, N., Ishimura, K., Sakamoto, H., Ogi, Y. and Miyazaki, Y.: A Design Method for a Space Antenna Structure Consisting of Radial Ribs and Hoop Cables, Proceedings of 24th JSME Computational Mechanics Conference CMD2011, No. 2326 (2011), pp. 687-688. (in Japanese)
- 3) Miyazaki, Y. and Tanaka, H.: Elastica Solution for Simplified Model for a Space Antenna Structure Consisting of Radial Ribs and Hoop Cables, Proceedings of 24th JSME Computational Mechanics Conference CMD2011, No. 2327 (2011), pp. 689-690. (in Japanese)
- 4) Kogiso, N., Tanaka, H., Akita, T., Ishimura, K., Sakamoto, H., Ogi, Y., Miyazaki, Y. and Iwasa, T.: Comparison of Computation Accuracy in FEM Analysis for a Space Antenna Structural Design, Proceedings of 24th JSME Computational Mechanics Conference CMD2011, No. 2328 (2011), pp. 691-693. (in Japanese)
- 5) Sakamoto, H., Kogiso, N., Tanaka, H., Ishimura, K. and Okuma, M.: Finite-Element Model Updating for Highly Precise Tension-stabilized Space Reflectors, Proceedings of 53rd AIAA/ASME/ASCE/AHS/ASC Structures, Structural Dynamics, and Materials Conference, AIAA Paper 2012-1837, 2012.
- 6) Friswell, M. I. and Mottershead, J. E.: *Finite Element Model Updating in Structural Dynamics*, Kluwer Academic Publishers, Dordrecht, 1995.
- 7) Mottershead, J. E., Link, M. and Friswell, M.: The Sensitivity Method in Finite Element Model Updating: A Tutorial, *Mechanical Systems and Signal Processing*, **25** (2011), pp. 2275-2296.
- 8) Nakayama, H. and Sawaragi, Y.: Satisficing Trade-off Method for Multiobjective Programming, *Lecture Notes in Economics and Mathematical Systems*, **229** (1984), pp. 113-122.
- 9) Nakayama, H., Kaneshige, K., Takemoto, S. and Watada, Y.: An Application of a Multi-objective Programming Technique to Construction Accuracy Control of Cable-stayed Bridges, *European Journal of Operational Research*, **87**, (1995), pp. 731-738.
- 10) Toyoda, M. and Kogiso, N.: Robust Multiobjective Optimization Method Using Satisficing Trade-Off Method, *Journal of Mechanical Science and Technology*, **29**, (2015), pp. 1361-1367.
- 11) Kogiso, N., Kodama, R. and Toyoda, M.: Reliability-Based Multiobjective Optimization Using The Satisficing Trade-Off Method, *Mechanical Engineering Journal*, **1**, (2014), pp. DSM0063-1 - DSM0063-12.
- 12) Nakayama, H.: Trade-Off Analysis Using Parametric Optimization Techniques, *European Journal of Operational Research*, **60**, (1992), pp. 87-98.